Article

The Kinetic Stability of Cytochrome *c* Oxidase: Effect of Bound Phospholipid and Dimerization

Erik Sedlák,[1,*] Rastislav Varhač,[1] Andrej Musatov,[1] and Neal C. Robinson[1]
[1]Department of Biochemistry, The University of Texas Health Science Center, San Antonio, Texas

ABSTRACT Thermally induced transitions of the 13-subunit integral membrane protein bovine cytochrome *c* oxidase (CcO) have been studied by differential scanning calorimetry (DSC) and circular dichroism (CD). Thermal denaturation of dodecyl maltoside solubilized CcO proceeds in two consecutive, irreversible, kinetically driven steps with the apparent transition temperatures at ~ 51°C and ~ 61°C (5μM CcO at scan rate of 1.5 K/min). The thermal denaturation data were analyzed according to the Lyubarev and Kurganov model of two consecutive irreversible steps. However, because of the limitation of the model to describe the complex mechanism of the thermal denaturation of CcO, the obtained results were utilized only for comparison purposes of kinetic stabilities of CcO under specific protein concentration (5μM) and scan rate (1.5 K/min). This enabled us to show that both the amphiphilic environment and the self-association state of CcO affect its kinetic stability. Kinetic stabilities of both steps are significantly decreased when all of the phospholipids are removed from CcO by phospholipase A_2 (the half-life decreases at 37°C). Conversely, dimerization of CcO induced by sodium cholate significantly increases its kinetic stability of only the first step (the half-life increases at 37°C). Protein concentration-dependent nonspecific oligomerization also indicate mild stabilization of CcO. Both, reversed-phase high-performance liquid chromatography (HPLC) and SDS-PAGE subunit analysis reveal that the first step of thermal denaturation involves dissociation of subunits III, VIa, VIb, and VIIa, whereas the second step is less well defined and most likely involves global unfold and aggregation of the remaining subunits. Electron transport activity of CcO decreases in a sigmoidal manner during the first transition and this dependence is very well described by kinetic parameters for the first step of the thermal transition. Therefore, dissociation of subunit III and/or VIIa is responsible for temperature-induced inactivation of CcO because VIa and VIb can be removed from CcO without affecting the enzyme activity. These results demonstrate an important role of tightly bound phospholipids and oligomeric state (particularly the dimeric form) of CcO for kinetic stability of the protein.

INTRODUCTION

Bovine cytochrome *c* oxidase (CcO) (ferrocytochrome *c*: O_2 oxidoreductase; EC 1.9.3.1) is the terminal enzyme complex of the inner mitochondrial membrane electron transport chain and catalyzes electron transfer from reduced cytochrome *c* to molecular oxygen. CcO is a multisubunit protein consisting of 13 dissimilar subunits: the three mitochondrial-encoded subunits (I, II, III) that form the core of the enzyme and contain four metal centers (Cu_A, heme *a*, heme a_3, and Cu_B) and the 10 nuclear-encoded subunits that surround the core and are unique to mitochondrial terminal oxidases (1,2). The enzyme complex spans the inner mitochondrial membrane and is in contact with an annulus of membrane phospholipids. Isolated detergent-solubilized CcO contains three to four tightly bound cardiolipin molecules with an important role for stabilizing the quaternary structure and activity of the enzyme (3–6). CcO crystallizes in a dimer form, which is generally considered as the functional unit in the lipid bilayer. However, there is little information regarding the functional and structural significances of the dimeric form of CcO. We have shown previously that dimeric CcO is significantly more stable against the effect of hydrostatic pressure than the monomeric form suggesting a role for the quaternary structure in stabilizing the enzyme against environmental perturbations (7).

Although the most common environmental perturbation is temperature, information regarding factors affecting the thermal stability of integral membrane proteins is very limited (8–10). Lack of detailed information concerning this topic may be caused by protein delipidation issues, a poorly defined oligomeric state, and the complexity of analyzing irreversible thermal transitions. For example, harsh conditions have often been used during protein delipidation, which have lead to irreversible conformational changes and/or dissociation of subunits from multimeric proteins that preclude this type of analysis.

Submitted June 25, 2014, and accepted for publication October 22, 2014.

*Correspondence: erik.sedlak@upjs.sk

Erik Sedlák's present address is Centre for Interdisciplinary Biosciences, P. J. Šafárik University, Jesenná 5, 040 01 Košice, Slovakia and Department of Biochemistry, P. J. Šafárik University, Moyzesova 11, 040 01 Košice, Slovakia.

Rastislav Varhač's present address is Department of Biochemistry, P. J. Šafárik University, Moyzesova 11, 040 01 Košice, Slovakia.

Andrej Musatov's present address is Department of Biophysics, Institute of Experimental Physics, Watsonova 47, 040 01 Košice, Slovakia.

Editor: Heiko Heerklotz

0006-3495/14/12/2941/9 $2.00

http://dx.doi.org/10.1016/j.bpj.2014.10.055

We have developed a mild delipidation procedure for detergent-solubilized integral membrane proteins, such as CcO and cytochrome bc_1 complex, that do not cause irreversible conformational changes in the proteins because both can be reactivated by exogenous phospholipids (3,11). We also have developed a simple, robust, and reversible procedure for preparing monomeric and dimeric CcO by manipulating the amphiphilic environment surrounding the enzyme (12,13). This provides us with a unique opportunity to address the role of tightly bound phospholipids and the oligomeric state of CcO for its thermal stability. Moreover, available quantitative analysis of both mitochondrial and nuclear-encoded subunits enables us to describe in detail thermal denaturation of this multimeric enzyme.

MATERIALS AND METHODS

Materials

Dodecyl maltoside (DM) was purchased from Anatrace, Inc. (Maumee, OH) Sodium cholate and horse heart cytochrome *c* (type III) were purchased from Sigma Chemical Co.(St. Louis, MO). The C_{18} reversed phase high-performance liquid chromatography (HPLC) column (4.6 × 250 mm, 218TP104, 5 μm, 300 Å pore size) was purchased from Vydac (BGB Analytik, Alexandria, VA). The HiTrap Q FPLC column (Q Sepharose HP 1 mL) was obtained from Pharmacia Biotech (GE Healthcare Bio-Sciences, Pittsburgh, PA). Acetonitrile and phosphoric acid were of HPLC grade and were obtained from Fisher Scientific (Pittsburgh, PA). HPLC grade chloroform and methanol were from EM Science (Billerica, MA). Ultrapure DM was obtained from either Boehringer Mannheim (Mannheim, Germany) or Anatrace, Inc. All other chemicals were of analytical grade.

Cytochrome *c* oxidase purification

Bovine heart CcO was isolated from heart muscle particles as previously described (14). The final enzyme precipitate was solubilized at ~ 120 μM heme aa_3 in 0.1 M NaH_2PO_4 buffer (pH 7.4) containing 25 mM sodium cholate and 1.0 mM EDTA, frozen as ~ 50 μL aliquots in liquid nitrogen, and stored at -80°C until used. The purified enzyme contained 9.5 to 10 nmol of heme A per mg of protein and had a molecular activity of 380 to 400 s^{-1} when assayed spectrophotometrically with 0.025 M phosphate buffer (pH 7.2) containing 2 mM DM, with 25 to 30 μM ferrocytochrome *c* as the substrate. Before each experiment, the frozen aliquots were thawed and DM substituted for the sodium cholate in the enzyme preparation by diluting the enzyme to 1 mg/mL with 1 mg/mL DM, followed by removal of sodium cholate by extensive dialysis against buffer containing greater than critical micelle concentration (CMC) concentrations of the new detergent. The resulting DM-solubilized enzyme was monomeric as judged by sedimentation velocity analysis (12,15,16). CcO concentrations were calculated based on $\varepsilon_{422} = 1.54 \times 10^5$ M^{-1} cm^{-1} (17). Reduced horse heart ferrocytochrome c ($\varepsilon_{550} = 29.5$ mM^{-1} cm^{-1}) for activity measurements was freshly prepared by dithionite reduction followed by Sephadex G-25 gel filtration for removal of excess dithionite.

Delipidation of cytochrome *c* oxidase

Phospholipid-free (PL-free) CcO phospholipase A_2 digestion of protein-bound phospholipids was followed by HiTrap Q FPLC to remove the resulting lysoPL and free fatty acids as described previously (3). CcO (usually 5 μM) was delipidated by incubation with an equimolar concentration of PLA_2 for 2 hr at room temperature in 20 mM MOPS (3-(N-morpholino) propanesulfonic acid), pH 7.2 containing 20% glycerol, 10 mM $CaCl_2$, and 1 mg detergent (DM or Triton X-100) per mg CcO. The reaction was stopped by addition of final concentration of 50 mM EDTA. PL-free CcO was purified by HiTrap Q column as previously described (3).

HiTrap Q FPLC anion-exchange column chromatography

Intact, PLA_2-delipidated CcO, or their thermal-induced subunit-depleted subcomplexes were purified by sodium sulfate gradient elution from a HiTrap Q anion-exchange column in 20 mM MOPS, pH 7.2, containing 2 mM DM. The equipment and protocol for the FPLC anion-exchange chromatographic separation of subunit depleted forms of CcO were described by Sedlák and Robinson (3).

Subunit analysis by reversed-phase HPLC and SDS-PAGE

The subunit content of the three HiTrap Q FPLC purified forms of CcO was quantified by C_{18} reversed-phase HPLC and SDS-PAGE (Sodium Dodecyl Sulfate PolyAcrylamide Gel Electrophoresis) as previously described (3,18,19). The 10 nuclear-encoded subunits were quantified using the reversed-phase HPLC method after normalizing each elution peak area assuming a constant yield for subunit Va (association of subunit Va is unaffected by exposure to 52°C or 54°C of PL-free or phospholipid-containing (PL-containing) CcO, respectively). The content of the three mitochondrially encoded subunits was determined after resolution by SDS-PAGE using a 15% acrylamide running gel containing 2 M urea and 0.1% SDS (18). The image of the Coomassie Blue G-250-stained gel was captured using a Bio-Rad GS-800 calibrated densitometer and the intensity of each band quantified using NIH ImageJ version 1.37.

Circular dichroism measurements

Circular dichroism (CD) spectra in the far-UV range (190 to 260 nm) were recorded on a Jasco-810 instrument with cell path of 1 mm and protein concentration of 0.4 μM. Each spectrum was an average of 10 scans. All spectra were background-corrected. The thermal CD experiments were monitored at 222 nm using a constant heating rate of 1.5 K/min. For determination of apparent transition temperatures for the two-step thermal transition, observed by molar ellipticity at 222 nm, the following equation for a two-step equilibrium transition was used:

$$\theta = \frac{\theta_N + \theta_I e^{-(\Delta H_1/(1-T/T_{m1}))/(RT)} + \theta_D e^{-(\Delta H_1/(1-T/T_{m1})+\Delta H_2/(1-T/T_{m2}))/(RT)}}{1 + e^{-(\Delta H_1/(1-T/T_{m1}))/(RT)} + e^{-(\Delta H_1/(1-T/T_{m1})+\Delta H_2/(1-T/T_{m2}))/(RT)}}, \quad (1)$$

where θ is the observed ellipticity; θ_N, θ_I, and θ_D are the molar ellipticities of native, intermediate, and denatured states, respectively; ΔH_1 and ΔH_2 are apparent enthalpies of the first and the second transitions, respectively; and

T_{m1} and T_{m2} are apparent temperatures of transitions of the first and the second steps, respectively.

Differential scanning calorimetry

DSC experiments were performed on a VP-DSC differential scanning microcalorimeter (Microcal, Northampton, MA) at a scan rate of 1.5 K/min. Protein concentration was, if not stated otherwise, 5 μM in 20mM TrisHCl, pH 8.0. Before each measurement, the sample and reference solutions were degassed in an evacuated chamber for 5 min at room temperature and carefully loaded into exhaustively cleaned cells using care to avoid bubble formation. A pressure of 2 atm was kept in the cells throughout the heating cycles to prevent degassing. A background scan, collected with buffer in both cells, was subtracted from each sample scan. The reversibility of the transitions was assessed by the reproducibility of the calorimetric trace in a second heating cycle performed immediately after cooling from the first scan. Excess heat capacity curves were plotted using Origin software supplied by Microcal.

DSC data analysis

DSC-monitored thermal denaturation of CcO (at scan rates of 1.0 and 1.5 K/min) consists of two consecutive irreversible steps that can be (in first approximation) described by the following scheme:

$$N \xrightarrow{k_1} I \xrightarrow{k_2} D, \tag{2}$$

where N, I, and D are native, intermediate, and denatured states, respectively; and k_1 and k_2 are rate constants of corresponding reactions. Analysis of DSC data using the model of two consecutive irreversible steps has been described in detail by Lyubarev and Kurganov (20). Briefly, the kinetic behavior of the system is described by the following differential equations:

$$\frac{d\gamma_N}{dt} = -k_1\gamma_N, \tag{3}$$

$$\frac{d\gamma_I}{dt} = k_1\gamma_N - k_2\gamma_I, \tag{4}$$

where γ_N and γ_I are the mole fractions of native and partially unfolded protein, respectively. The rate constants at any given temperature can be obtained from the Arrhenius equation, in alternative form:

$$k = \exp\left[\frac{E_a}{R}\left(\frac{1}{T^*} - \frac{1}{T}\right)\right], \tag{5}$$

where E_a is the energy of activation, R is the gas constant, and the parameter T^* equals to temperature at which rate constant equals 1 min^{-1}. After substituting $dt = dT/\nu$, where ν is the scan rate, and solving the equations, the following is obtained:

$$\gamma_N = \exp\left(-\frac{1}{\nu}\int_{T_0}^{T} k_1 dT\right), \tag{6}$$

$$\gamma_I = \frac{1}{\nu}\exp\left(-\frac{1}{\nu}\int_{T_0}^{T} k_2 dT\right)\int_{T_0}^{T}\left[k_1\exp\left(\frac{1}{\nu}\int_{T_0}^{T}(k_2 - k_1)dT\right)\right]dT. \tag{7}$$

The excess heat capacity, which is the parameter measured in the DSC experiments, is then expressed by the following:

$$C_p^{exp} = \frac{d\langle\Delta H\rangle}{dT} = \frac{\Delta H_{u1}k_1}{\nu}\gamma_N + \frac{\Delta H_{u2}k_2}{\nu}\gamma_I, \tag{8}$$

where ΔH_{u1} and ΔH_{u2} are molar enthalpy changes for the first and second steps, respectively. The rate constants, k, are related to E_a and T^* via Eq. 5.

Dependence of CcO activity on temperature

DM-solubilized 5 μM CcO in phosphate buffer pH 7.2 was heated at the same rate as in the DSC experiment. At 5°C intervals, a 10 μL aliquot was removed and diluted with 190 μL ice-cold buffer. Activity was measured as described previously (3).

RESULTS

Thermal denaturation of CcO

Thermal denaturation of CcO (5 μM) was monitored by DSC at scan rates of 0.5, 1.0, and 1.5 K/min (Fig. 1). Two distinct cooperative thermal transitions occur at moderately fast scan rates of 1.0 or 1.5 K/min. The first transition, which has a lower amplitude for the molar heat capacity occurs at ~ 51°C (50.1°C and 51.6°C for the two scan rates, respectively); the second, with a higher amplitude, occurs at ~ 61°C (60.5°C and 61.6°C, respectively). However, at a slower scan rate of 0.5 K/min, the CcO thermal transitions are complex with asymmetrical transitions. For example, the second transition at ~ 60°C has a leading shoulder at ~ 55°C indicating another (third) temperature-induced transition. In all cases, both the first and the second thermal transitions were judged to be irreversible because no transitions were obtained upon cooling and rescanning the sample. If the

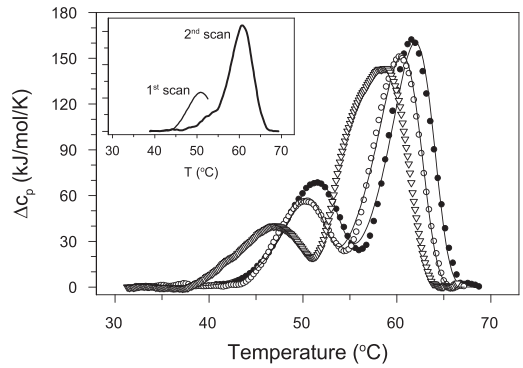

FIGURE 1 Thermal transitions of PL-containing CcO as monitored by DSC. Measurements were performed at three different scan rates: 0.5 K/min (*open triangles*), 1.0 K/min (*open circles*), and 1.5 K/min (*solid circles*); theoretical fits based on Eq. 8 are shown as solid lines. The dependence of the thermal transition temperatures on the scan rate indicates that thermal denaturation of CcO is under kinetic control. Inset: DSC scan of CcO heated at a scan rate of 1.5 K/min until 54°C (*first scan, thin line*), recooled to 25°C, and rescanned at the same scan rate (*second scan, thick line*). The fact that the first thermal transition is absent during the second scan indicates the irreversibility of the first thermal CcO transition. All DSC experiments used 5 μM CcO solubilized in 2 mM DM in 20 mM TrisHCl, pH 8.0.

protein solution is cooled after stopping the first scan at 54° K, i.e., after the first transition, but before the second, the solution remains clear; the results of a second rescanning of the sample are very different (inset, Fig. 1). Cooling of a sample that has been heated through both transitions produces a solution filled with protein aggregates.

Dependence of the transitions on scan rate of heating indicates that the thermally induced transitions within CcO are kinetically driven. The two consecutive irreversible transitions observed at high scan rates of 1.0 or 1.5 K/min can be described by Eq. 1 in the Materials and Methods section: $N \overset{k_1}{\rightarrow} I \overset{k_2}{\rightarrow} D$. However, the observation that the mechanism of thermal denaturation of CcO is more complex at scan rates slower than 1.0 K/min indicates that the Lyubarev and Kurganov model is not sufficiently robust and in our work can be used only for qualitative comparisons of kinetic stabilities of (PL-containing and PL-free) CcO measured at the same scan rate of 1.5 K/min and the same (5 μM) protein concentration. Each set of DSC data were fitted to Eq. 8, which yields the following six parameters reflecting a two-step, irreversible transition: ΔH_{u1}, ΔH_{u2}, E_{a1}, E_{a2}, T_1*, and T_2* (Table S1). The half-life or so-called shelf-life, τ, of CcO at 37°C was calculated as $\tau = ln2/k_1$, where k_1 was obtained from Eq. 5.

Loss of electron-transport activity of CcO during the thermal transitions

The dependence of the functional state of CcO on temperature was determined by monitoring electron transfer activity of the enzyme after it had been heated to a particular temperature and then cooled to prevent further structural or functional changes. At each temperature an aliquot was removed, cooled on ice, and the CcO activity was subsequently measured at 25°C. The experimental conditions were chosen to be as close as possible to those used for the DSC experiments, i.e., 5 μM CcO, 2 mM DM and a heating rate of 1.5 K/min. Near the first transition temperature, CcO activity decreased with increasing temperature in a sigmoidal way with a midpoint at ~ 52°C (Fig. 2) indicating that the loss of activity is associated with the first thermal transition at 51.6°C. In fact, the fraction of native protein, γ_N, as a function of temperature calculated using Eq. 6 and the parameters of Table S1 obtained from DSC measurements, closely correlates with the temperature dependence for the loss of CcO activity (Fig. 2). This result suggests that the first thermal transition is associated with conformational change(s) in CcO that are critical for its activity.

Effect of delipidation on kinetic stability of CcO

Removal of the phospholipids that copurify with detergent-solubilized CcO perturbs the kinetic stability of CcO as is evident from the shift in both thermal transitions to lower temperature (Fig. 3). Both the calorimetric enthalpies

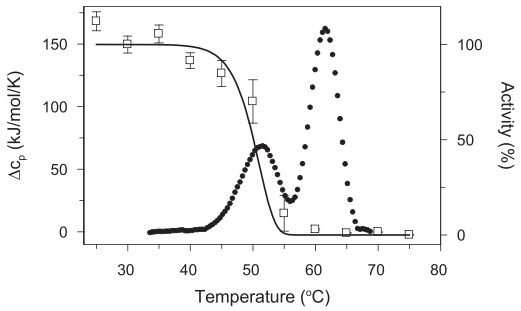

FIGURE 2 Comparison of the temperature dependence of CcO activity with the DSC-monitored thermal transitions. Experimental data are shown as symbols: DSC (*solid circles*) and CcO activity (*open squares*). The solid line represents the percent of the native state population, γ_N, calculated using Eq. 6 and the parameters obtained from fitting of the DSC thermal transition data. The coincident decrease of CcO activity and the population of the CcO native state indicate that temperature-induced conformational changes occurring during the first thermal transition are critical for CcO activity. The measurements were performed at the same conditions as described in Fig. 1.

(ΔH_{u1} and ΔH_{u2}) and the apparent transition temperatures (T_1 and T_2) were smaller and shifted to lower temperatures, respectively (Table S1). The half-life of CcO at a particular temperature can be estimated from the experimental parameters used to fit the experimental DSC data together with Eq. 8. With this approach, the half-life of PL-free CcO at 37°C was found to be ~ 20 times shorter than for PL-containing CcO, i.e., ~ 0.4 h versus ~ 8 h.

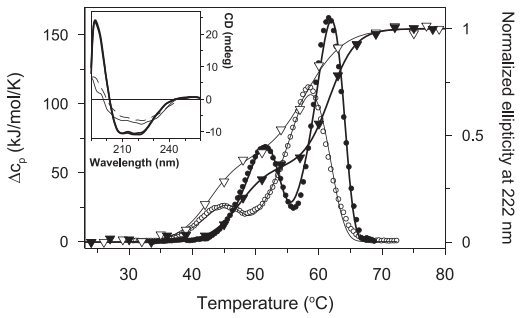

FIGURE 3 Comparison of thermal transitions of CcO as monitored by CD and DSC. Experimental data are shown as symbols: PL-containing CcO (*solid symbols*), PL-free CcO (*open symbols*), DSC data (*circles*), and CD data (*triangles*). Theoretical fits to CD and DSC data (*solid lines*) are based on Eqs. 1 and 8, respectively. Fits are shown for both PL-containing CcO (*thick line*) and PL-free CcO (*thin line*). The fraction unfolded as monitored by CD were normalized to vary between 0 and 1 as the temperature was raised from 0°C to 80°C (see inset figure). Removal of bound phospholipid from CcO shifts both thermal transitions to lower temperatures, whether monitored by CD or DSC. Inset: CD spectra of PL-containing CcO (*solid lines*) and PL-free CcO (*dashed lines*) measured at either 25°C (*thick lines*) or 80°C (*thin lines*). CD spectra of both CcO forms at 25°C are overlapping. CD spectra at 80°C indicate that 50% to 60% of the native secondary structure remains in the thermally denatured states of both forms of CcO. DSC and CD experiments were performed using 5 μM CcO solubilized in 20 mM TrisHCl, pH 8.0 containing 2 mM DM at a scan rate of 1.5 K/min.

Thermally induced structural transitions within PL-containing and PL-free CcOs are also apparent from the temperature dependence of the molar ellipticity at 222 nm. Temperature-induced changes in ellipticity of both PL-containing and PL-free CcO indicate two sequential steps with transitions at 47.9°C and 61.7°C for PL-containing CcO and transitions at 42.7°C and 58.2°C for the PL-free CcO (evaluated using Eq. 1). The transitions temperatures obtained from these CD experiments are quite similar with those obtained from the DSC measurements (Table S1). The transition temperatures obtained from the CD measurements, ~ 3°C lower, suggest that perturbation of the secondary structure occurs at slightly lower temperatures than the structural transitions detected by DSC. CD spectra of thermally denatured PL-containing, or PL-free CcO, i.e., after heating to 80°, indicate that ~ 50% to 60% of their secondary structure remains (inset in Fig. 3), similar to results obtained with *Paracoccus denitrificans* CcO (21).

The quaternary structure of PL-containing and PL-free CcO at temperatures corresponding to the two thermal transitions were quantified using C_{18} reversed-phase HPLC and SDS-PAGE after removal of dissociated subunits using gradient elution by HiTrap Q FPLC anion-exchange chromatography. HiTrap Q FPLC separates intact CcO from its subunit-depleted complexes (3,7; Fig. 4). At pH 7.2, 80% to 85% of DM-solubilized CcO elutes as an intact, 13-subunit complex (peak A), whereas the remaining 15% to 20% elutes as the 11-subunit complex (peak B).

Subunit analysis of individual peaks by reversed phase C_{18} HPLC chromatography (Fig. 5) and gel electrophoresis (inset in Fig. 5) confirms our previous results (3,7); peaks A, B, and C correspond to the 13-, 11-, and 9-subunit forms CcO, respectively. The 11-subunit form of CcO is missing subunits VIa and VIb; the 9-subunit form of CcO is missing subunits III, VIa, VIb, and VIIa. These results are in good agreement with previous studies in which the subunit content of thermally denatured CcO was obtained utilizing the different solubility properties of thermally denatured subunits (22,23).

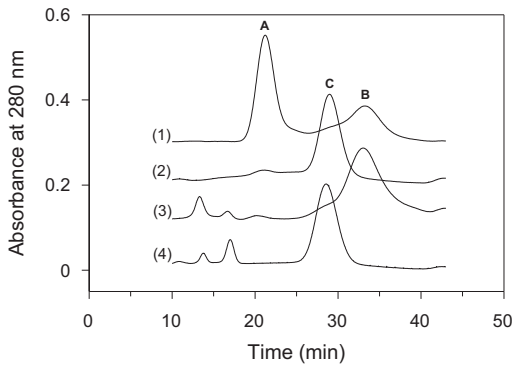

FIGURE 4 Analysis of PL-containing and PL-free CcO by HiTrap Q FPLC anion-exchange chromatography before and after they were heated through the first-step transition. Chromatograms (1) and (2) were obtained for PL-containing CcO before and after heating to 54°C followed by cooling to 23°C, respectively. Chromatograms (3) and (4) were obtained for PL-free CcO before and after it had been heated and cooled in an identical manner. CcO that eluted in peaks A, B, and C were collected and analyzed by reversed phase-HPLC (refer to Fig. 5).

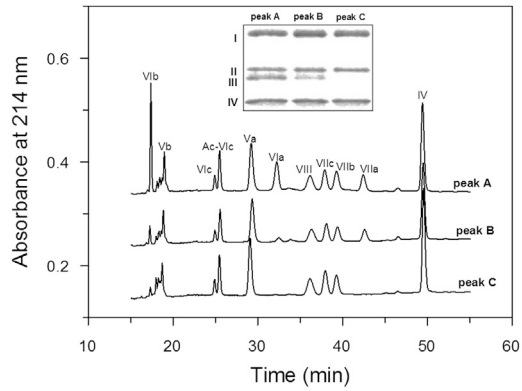

FIGURE 5 Subunit composition of CcO before and after the first thermal transition. Nuclear-encoded CcO subunits were analyzed by C_{18} reversed-phase HPLC (*main figure*); mitochondrial-encoded subunits were analyzed by SDS-PAGE (*inset*). Chromatograms labeled as peak A, B, and C represent HPLC of fractions collected under peaks A, B, and C from Fig. 4, respectively. Chromatograms for peaks A and B were those obtained for intact CcO (13-subunit form of CcO) and PL-free CcO (11-subunit form of CcO) before each being heated above 25°C. Chromatogram for peak C was that obtained for PL-containing CcO after it had been heated to 54°C. An identical chromatogram was obtained for peak C material obtained from PL-free CcO that had been heated to 52°C. Analysis of peak C material, whether it had been isolated from either PL-containing or PL-free, had an identical subunit composition. Inset: SDS-PAGE analysis of mitochondrial-encoded CcO subunits composition of intact, PL-containing CcO before (peaks A and B) and after heating to 54°C (peak C). Identical SDS-PAGE results were obtained for peak B and C material that had been isolated from PL-free CcO.

Kinetic stability of CcO increases with protein concentration

The kinetic stability of CcO depends on its concentration. This is indicated by a shift of both DSC thermal transitions, T_1 and T_2, to higher temperatures (corresponding to a position of maximum of change in molar thermal capacity) with higher protein concentration (Fig. 6, Table S2). Dependence of thermal denaturation on protein concentration suggests that CcO self-associates at higher protein concentration. This dependence indicates that CcO solubilized in DM before denaturation may form nonspecific aggregates. The reason of the tendency to form aggregates of CcO is likely strengthening of hydrophobic effect with increasing temperature (24). This is in agreement with the observed tendency of CcO to precipitate after thermal denaturation with increased protein concentration. Dependence of thermal denaturation on protein concentration confirms that the mechanism of thermal transitions of CcO is complex and cannot be properly described by the Lyubarev and Kurganov

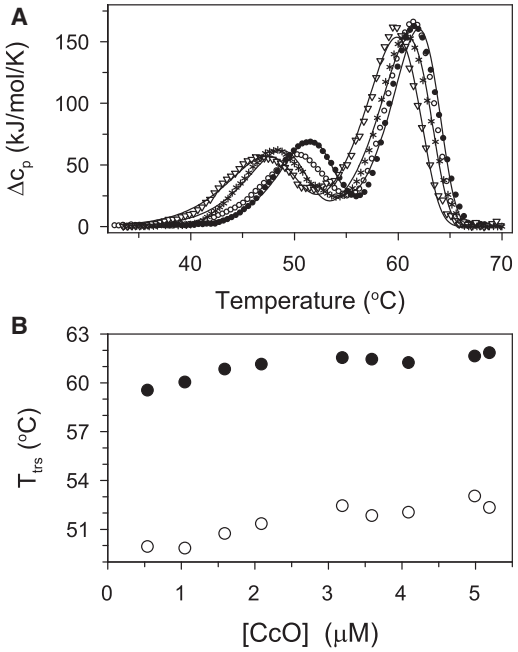

FIGURE 6 DSC scans and fitting parameters obtained for PL-containing CcO as a function of protein concentration. (*A*) DSC scans obtained with 0.55 μM (*triangles*), 1.6 μM (*asterisks*), 3.2 μM (*open circles*), and 5.0 μM (*solid circles*) CcO. (*B*) Dependence of aparent temperature, T_{trs}, of thermal transitions of the first (*open circles*) and the second step (*solid circles*) of thermal denaturation. In each case CcO was solubilized in 20 mM TrisHCl, pH 8.0 containing 2 mM DM, and the DSC data were acquired using a scan rate of 1.5 K/min.

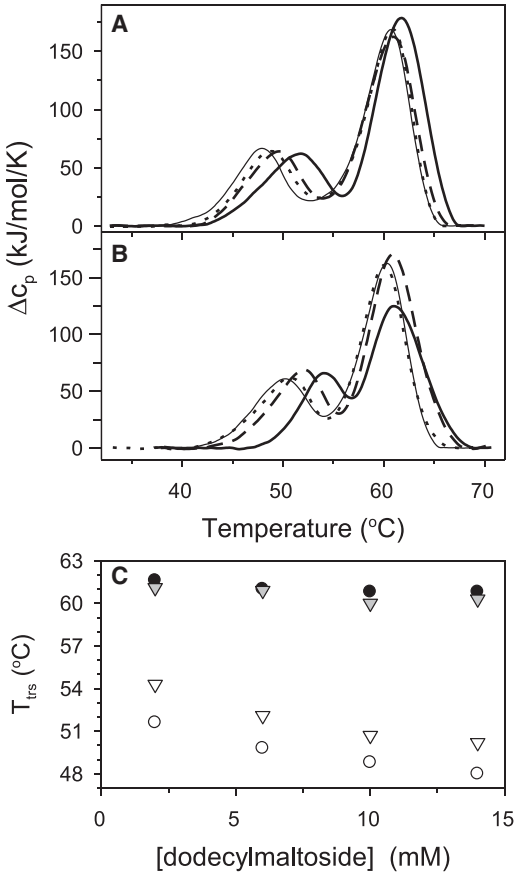

FIGURE 7 DSC scans obtained for PL-containing CcO in the absence (*A*) and in the presence (*B*) of 2 mM sodium cholate with increasing concentration of DM: 2 mM (*solid thick line*), 6 mM (*dashed*), 10 mM (*dotted*), and 14 mM (*solid thin*). (*C*) The DM dependence of the apparent transition temperature, T_{trs}, for the first (*open symbols*) and the second (*solid symbols*) stages of CcO thermal denaturation in the absence (*circles*) or presence (*triangles*) of 2 mM sodium cholate. All DSC data were acquired at a scan rate of 1.5 K/min using 5 μM phospholipid-containing CcO solubilized in 20 mM TrisHCl, pH 8.0 buffer containing the indicated concentration of DM and either 0 or 2 mM sodium cholate.

model. In fact, this model involving two kinetic steps described by first-order rate equations is unable to account for the observed protein concentration dependence. Therefore, the model was not applied on the DSC data obtained at different CcO concentrations. However, the model—independent parameters (transition temperatures and values of calorimetric enthalpies)—obtained from DSC transitions of CcO at different concentration of CcO at a scan rate of 1.5 K/min were calculated and listed in Table S2.

Dimerization stabilizes CcO

The effect of the quaternary structure, i.e., dimer versus monomer, on the kinetic stability of CcO was investigated by manipulating the percentage of dimeric CcO in solution. This can be done by inclusion of sodium cholate, which induces CcO dimer formation. The kinetic stability of dimeric CcO, containing two copies of each of the 13 CcO subunits, was compared with monomeric CcO, containing a single copy of each of the 13 CcO subunits (Fig. 7). Both sets of experiments were also done as a function of increasing the DM concentration, i.e., 6, 10, and 14 mM (Fig. 7 and Table S3). Increasing the DM concentration, either in the presence or absence of sodium cholate, induces the monomeric form of CcO as was demonstrated previously by sedimentation analysis (13). The presence of 2 mM sodium cholate has a significant stabilization effect on the first CcO thermal transition whereas the second step is relatively unaffected (Fig. 7 *C*). The half-life of the CcO dimer at 37°C, i.e., oxidase that is solubilized in 2 mM DM in the presence of 2 mM sodium cholate, is ~ 65 times longer than the monomeric form of the protein (in the absence of sodium cholate). Increasing DM concentration, however, destabilizes CcO. The destabilization effect is probably attributable to two factors: 1), in the presence of sodium cholate, increasing DM concentration would be expected to decrease the percentage of dimer because of dilution of the cholate effect; 2), in the absence of sodium cholate, increasing DM concentration probably decreases the affinity of subunits for the core of CcO, which decreases its kinetic stability. Supporting evidence for the latter is the fact that prolonged exposure of CcO to high concentrations of detergent often depletes the enzyme of subunits VIa and VIb.

DISCUSSION

DSC was used to probe the effect of bound phospholipid and oligomerization on the thermal stability of bovine heart CcO solubilized in DM. In contrast to small monomeric water-soluble proteins, temperature-induced thermal transitions in CcO are complex and irreversible. The complexity arises from the fact that detergent-solubilized CcO is a multimeric intrinsic membrane protein complex comprised of 13 dissimilar subunits that contains 15 to 30 bound phospholipids. Furthermore, the protein-phospholipid complex dimerizes, the extent of which depends on the composition and concentration of the solubilizing detergent (12,13). The irreversibility of the thermal transitions, together with the dissociation of subunits, further complicates interpretation of the data. Two consecutive, irreversible transitions of CcO observed at high scan rates allowed us to test the Lyubarev and Kurganov model for analysis of the acquired DSC data (refer to Eq. 2 in Materials and Methods). However, detailed examination of the thermal denaturation of CcO revealed that the model is only of limited use in our experiments. This is because: (1), it does not describe the DSC transitions in a substantial range of scan rates, and (2), it does not explain the experimentally observed protein concentration effect on thermal denaturation. Therefore, the model was only used for comparative purposes and to fit the DSC profiles obtained at a high scan rate of 1.5 K/min, and the concentration of protein was always 5 μM.

The present study is an attempt to address the kinetic stability of a large, multimeric, intrinsic membrane protein complex such as CcO. Our results indicate that the kinetic stability of DM-solubilized CcO is significantly influenced by both the amount of bound phospholipid and oligomerization of the 13-subunit monomeric unit. Furthermore, the irreversibility of the sequential kinetic steps has allowed us to identify which subunits dissociate during each of the transitions.

Sequential dissociation of subunits in the process of thermal denaturation of dodecyl maltoside-solubilized CcO

Thermal denaturation of either phospholipid-containing, or phospholipid-free CcO proceeds in two consecutive irreversible steps, both of which are under kinetic control (Fig. 1). The existence of two consecutive irreversible transitions during thermal denaturation of PL-containing CcO has been previously described for mammalian mitochondrial CcO (22,23,25,26), yeast mitochondrial CcO (27), and bacterial CcO (21). Freire's group (22,23) attempted to correlate the thermal transitions occurring within bovine CcO to the dissociation of individual subunits; however, their analytical approach (differential detergent solubility of core CcO and its subunits (23) combined with SDS-PAGE (22) only permitted them to assign the dissociation of subunits III and VIa to the first step. The change in solubility of a dissociated subunit(s) after a thermally-induced transition is probably insufficient for detection of all subunits that dissociate from the core of the enzyme. We utilized two chromatographic steps that made it much easier to quantify the content of subunits associated with the core of CcO: anion-exchange HiTrap Q chromatography (Fig. 4) combined with quantitative subunit analysis by reversed phase C_{18} HPLC (Fig. 5). The first chromatographic step removes all subunits that have dissociated from the core of the enzyme after each of the irreversible thermal transitions. The second step, reversed phase C_{18} HPLC chromatography of the purified CcO, quantifies the subunit content of the CcO core. By this approach we were able to conclude that the first thermal transition for phospholipid-containing CcO occurs coincident with dissociation of subunits III, VIa, VIb, and VIIa. With phospholipid-free CcO the first transition involves only the dissociation of subunits III and VIIa since subunits VIa and VIb dissociate during the removal of tightly bound phospholipid (3). In addition, our results demonstrate that the first step of the thermal denaturation of either form of CcO is accompanied by: 1), a complete loss of enzymatic activity (Fig. 2); and 2), a decrease in molar ellipticity (Fig. 3). The first indicates a significant perturbation near the enzyme active sites; the second, at least a partial unfolding of the secondary structure, most likely within the dissociated subunits.

Examination of three-dimensional structure of CcO indicates that all four of the subunits that dissociate from CcO during the first thermal transition are located near the dimer interface and are in close contact with each other. The same four subunits, i.e., subunits III, VIa, VIb, and VIIa, also dissociate from the core of the enzyme during structural perturbations induced by either high hydrostatic pressure (7), or chemical denaturants, e.g., urea or guanidinium chloride (28). Removal of subunits VIa and VIb is known to have little effect on the electron transport activity of CcO (3); therefore, the temperature-induced loss of enzymatic activity must be caused by dissociation of subunit III and/or VIIa, or conformational changes induced in the CcO core as a consequence of their dissociation. This interpretation is in agreement with our previous conclusions derived from the loss of activity during exposure to either high hydrostatic pressure (7), or chemical denaturants (E. Sedlak and N. C. Robinson, unpublished results). In each case, the loss of enzymatic activity closely correlates with dissociation of subunits III and/or VIIa. Dissociation of subunit VIIa has also been suggested to be responsible for hydrogen peroxide–induced inhibition of CcO (29).

Phospholipid removal decreases kinetic stability of CcO

Comparison of DSC scans of phospholipid-containing and phospholipid-free CcO illustrates the stabilization effect

of bound phospholipid, probably attributable to tightly bound cardiolipin (Fig. 3). The two thermal transitions consist of several processes, including subunit dissociations (previously discussed) and possible partial unfolding of secondary and tertiary structures. Kinetic analysis (with discussed limitations) of our data provides a different picture regarding the role of phospholipid on protein stability than had been deduced from previous analyses based on equilibrium thermodynamic methods. The small shift to lower temperatures in both apparent transition temperatures (~ 3°C to 6°C) indicates only a mild destabilization effect upon removal of bound phospholipid. However, parameters obtained using the Lyubarev and Kurganov model and Eqs. 2 to 8 (Table S1) indicate that tightly bound phospholipids/cardiolipins significantly increases the kinetic stability of CcO since the half-life of phospholipid-containing CcO is ~ 20-fold longer at 37°C than is phospholipid-free CcO. Phospholipid removal itself has little affect on either the electron transport activity or the secondary structure of CcO provided the temperature is not raised through the first thermal transition (inset Fig. 3) (3). However, the phospholipid-free CcO is devoid of proton pumping activity, which suggests a significant structural perturbation of one or both of the proton channels into the active site upon phospholipid removal (30). Few studies address the effect of phospholipid removal on the stability of purified membrane proteins making it difficult to conclude that this is a general property of detergent-solubilized membrane proteins. However, complete or partial delipidation of other integral membrane proteins such as LH/hCG receptors (8), bacteriorhodopsin (9), purple bacterial reaction center (10), and bacterial CcO (A. Musatov et al., unpublished results) are accompanied by only a small destabilization effect as judged by the rather small decreases in their apparent thermal transition temperatures (decreases of 0°C to 5°C), findings that are similar with those observed in this study for CcO.

Effect of oligomeric state on kinetic stability of CcO

Conditions that favor dimerization of DM-solubilized CcO, i.e., inclusion of cholate or other bile salts, significantly increase the kinetic stability of CcO (Fig. 7 and Table S3). In the presence of cholate, the first transition is shifted to a slightly higher temperature, i.e., ~ 3°C, which indicates stabilization of CcO during the first transition. The effect is much more evident when examining the kinetic stability of the CcO dimer. The half-life of dimeric CcO is ~ 65-fold longer at 37°C compared with the half-life of monomeric CcO (Table S3). Since all of the subunits that dissociate during the first transition participate in the monomer-monomer contacts at the dimer interface, it is reasonable that dimerization has a significant stabilization effect. It is also reasonable that dimerization has little effect on the second transition. Once subunits III, VIa, VIb, and VIIa dissociate during the first transition, CcO could no longer form the normal protein contacts at the dimer interface, and the second transition would proceed identically, regardless of the original oligomeric state.

Dependence of transition temperature on protein concentration also indicates the importance of the oligomeric state on the kinetic stability and thermal denaturation of CcO (Fig. 6). Because the DM is kept constant as the protein concentration is raised, i.e., the detergent/protein ratio decreases as the protein concentration is increased, such self-association is similar with that observed by analytical ultracentrifugation at low detergent concentration (12). Despite the clear stabilization effect of oligomerization, self-association of CcO is likely the result of nonspecific interactions of CcO monomers and dimers. This conclusion is based on the observations that 1), oligomerization continually increases with protein concentration within a relatively small concentration range, and 2), both the lower and higher CcO thermal transitions are protein concentration dependent (Fig. 6). For the second transition to be stabilized, the contacts would have to be via the outer surface of CcO to be unaffected by dissociation of subunits III, VIa, VIb, and VIIa.

The present study is in agreement with all of our previous studies, i.e., 1), phospholipid removal alters not only association of specific subunits within CcO, but also decreases the kinetic stability of the entire protein complex; and 2), the dimeric state of CcO stabilizes the quaternary structure of CcO against the effects of increasing temperature. We, therefore, conclude that the kinetic stability of mitochondrial electron transport complex IV, CcO, is significantly enhanced by at least two factors that are important structural components: 1), bound phospholipid, and 2), CcO's oligomeric state. We also propose that this conclusion regarding the kinetic stability of CcO may be applicable to other multisubunit membrane proteins, although such a hypothesis must, of course, be verified by similar studies on other integral membrane proteins.

SUPPORTING MATERIAL

Three tables and experimentally determined and calculated parameters obtained for the data shown in Figures 1, 6 and 7 are available at http://www.biophysj.org/biophysj/supplemental/S0006-3495(14)01143-6.

AUTHOR CONTRIBUTIONS

Erik Sedlák and Rastislav Varhač contributed equally to this work.

This work was supported by a research grant from National Institute of General Medical Sciences (NIGMS 024795), by grants from the Slovak Grant Agency VEGA (projects No. 1/0521/12 & 2/0062/14) and from CELIM (316310) funded by 7FP EU (REGPOT).

REFERENCES

1. Kadenbach, B., J. Jarausch, …, P. Merle. 1983. Separation of mammalian cytochrome *c* oxidase into 13 polypeptides by a sodium dodecyl sulfate-gel electrophoretic procedure. *Anal. Biochem.* 129:517–521.
2. Tsukihara, T., H. Aoyama, …, S. Yoshikawa. 1996. The whole structure of the 13-subunit oxidized cytochrome *c* oxidase at 2.8 A. *Science.* 272:1136–1144.
3. Sedlák, E., and N. C. Robinson. 1999. Phospholipase A(2) digestion of cardiolipin bound to bovine cytochrome c oxidase alters both activity and quaternary structure. *Biochemistry.* 38:14966–14972.
4. Sedlák, E., M. Panda, …, N. C. Robinson. 2006. Photolabeling of cardiolipin binding subunits within bovine heart cytochrome *c* oxidase. *Biochemistry.* 45:746–754.
5. Shinzawa-Itoh, K., H. Aoyama, …, S. Yoshikawa. 2007. Structures and physiological roles of 13 integral lipids of bovine heart cytochrome *c* oxidase. *EMBO J.* 26:1713–1725.
6. Arnarez, C., S. J. Marrink, and X. Periole. 2013. Identification of cardiolipin binding sites on cytochrome *c* oxidase at the entrance of proton channels. *Sci. Rep.* 3:1263.
7. Stanicová, J., E. Sedlák, …, N. C. Robinson. 2007. Differential stability of dimeric and monomeric cytochrome *c* oxidase exposed to elevated hydrostatic pressure. *Biochemistry.* 46:7146–7152.
8. Kolena, J., S. Scsuková, and M. Jezová. 2002. Thermal destabilization of ovarian LH/hCG receptors by negatively charged lipids. *Exp. Clin. Endocrinol. Diabetes.* 110:77–79.
9. Heyes, C. D., and M. A. El-Sayed. 2002. The role of the native lipids and lattice structure in bacteriorhodopsin protein conformation and stability as studied by temperature-dependent Fourier transform-infrared spectroscopy. *J. Biol. Chem.* 277:29437–29443.
10. Fyfe, P. K., N. W. Isaacs, …, M. R. Jones. 2004. Disruption of a specific molecular interaction with a bound lipid affects the thermal stability of the purple bacterial reaction centre. *Biochim. Biophys. Acta.* 1608:11–22.
11. Gomez, Jr., B., and N. C. Robinson. 1999. Phospholipase digestion of bound cardiolipin reversibly inactivates bovine cytochrome bc_1. *Biochemistry.* 38:9031–9038.
12. Musatov, A., J. Ortega-Lopez, and N. C. Robinson. 2000. Detergent-solubilized bovine cytochrome *c* oxidase: dimerization depends on the amphiphilic environment. *Biochemistry.* 39:12996–13004.
13. Musatov, A., and N. C. Robinson. 2002. Cholate-induced dimerization of detergent- or phospholipid-solubilized bovine cytochrome c oxidase. *Biochemistry.* 41:4371–4376.
14. Mahapatro, S. N., and N. C. Robinson. 1990. Effect of changing the detergent bound to bovine cytochrome c oxidase upon its individual electron-transfer steps. *Biochemistry.* 29:764–770.
15. Robinson, N. C., and L. Talbert. 1986. Triton X-100 induced dissociation of beef heart cytochrome *c* oxidase into monomers. *Biochemistry.* 25:2328–2335.
16. Robinson, N. C., B. Gomez, …, J. Ortega-Lopez. 1998. Analysis of detergent solubilized membrane proteins in the analytical ultracentrifuge. *Chemtracts: New York.* 11:960–968.
17. van Gelder, B. F. 1978. Optical properties of cytochromes from beef heart mitochondria, submitochondrial vesicles, and derived preparations. *Methods Enzymol.* 53:125–128.
18. Robinson, N. C., F. Strey, and L. Talbert. 1980. Investigation of the essential boundary layer phospholipids of cytochrome c oxidase using Triton X-100 delipidation. *Biochemistry.* 19:3656–3661.
19. Liu, Y.-Ch., L. H. Sowdal, and N. C. Robinson. 1995. Separation and quantitation of cytochrome *c* oxidase subunits by mono-Q fast liquid chromatography and C18 reverse-phase high-performance liquid chromatography. *Arch. Biochem. Biophys.* 324:135–142.
20. Lyubarev, A. E., and B. I. Kurganov. 1998. Modeling of irreversible thermal protein denaturation at varying temperature. I. The model involving two consecutive irreversible steps. *Biochemistry Mosc.* 63:434–440.
21. Haltia, T., N. Semo, …, E. Freire. 1994. Thermodynamic and structural stability of cytochrome *c* oxidase from Paracoccus denitrificans. *Biochemistry.* 33:9731–9740.
22. Rigell, C. W., C. de Saussure, and E. Freire. 1985. Protein and lipid structural transitions in cytochrome *c* oxidase-dimyristoylphosphatidylcholine reconstitutions. *Biochemistry.* 24:5638–5646.
23. Rigell, C. W., and E. Freire. 1987. Differential detergent solubility investigation of thermally induced transitions in cytochrome *c* oxidase. *Biochemistry.* 26:4366–4371.
24. Privalov, P. L., and S. J. Gill. 1988. Stability of protein structure and hydrophobic interaction. *Adv. Protein Chem.* 39:191–234.
25. Yu, C. A., S. H. Gwak, and L. Yu. 1985. Studies on protein-lipid interactions in cytochrome *c* oxidase by differential scanning calorimetry. *Biochim. Biophys. Acta.* 812:656–664.
26. Musatov, A., E. A. Permyakov, …, V. I. Snyrov. 1990. Some aspects of fluorescence and microcalorimetric studies of cytochrome c oxidase. *Biochem. Int.* 21:563–571.
27. Morin, P. E., D. Diggs, and E. Freire. 1990. Thermal stability of membrane-reconstituted yeast cytochrome *c* oxidase. *Biochemistry.* 29:781–788.
28. Sedlák, E., and N. C. Robinson. 2009. Sequential dissociation of subunits from bovine heart cytochrome *c* oxidase by urea. *Biochemistry.* 48:8143–8150.
29. Musatov, A., E. Hebert, …, N. C. Robinson. 2004. Specific modification of two tryptophans within the nuclear-encoded subunits of bovine cytochrome *c* oxidase by hydrogen peroxide. *Biochemistry.* 43:1003–1009.
30. Musatov, A., and N. C. Robinson. 2014. Bound cardiolipin is essential for cytochrome *c* oxidase proton translocation. *Biochimie.* 105: 159–164.

The Kinetic Stability of Cytochrome *c* Oxidase: Effect of Bound Phospholipids and Dimerization

Erik Sedlák, Rastislav Varhač, Andrej Musatov, and Neal C. Robinson

Table S1. Calculated parameters based on two-step analysis of the data shown in Figure 1 the irreversible thermal transitions of PL-containing and PL-free CcO's at 5μM.

CcO form	E_{a1} *(kJ/mol)*	T_1^*/T_1 *(°C)*	ΔH_{u1} *(kJ/mol)*	$\tau_{37\ degC}$ *(hours)*	E_{a2} *(kJ/mol)*	T_2^*/T_2 *(°C)*	ΔH_{u2} *(kJ/mol)*	R^2
PL-containing	344	53.0/51.6	504	8.0	413	63.2/61.6	1157	0.9917
1.5 K/min	±10	±0.1	±11		±5	±0.1	±12	
PL-free CcO	283	47.1/45.2	198	0.4	268	61.8/58.4	1097	0.9934
1.5 K/min	±14	±0.3	±8		±3	±0.1	±10	

*T** values are the temperatures at which the rate constant for the specific reaction is 1/min. *T* values are the temperatures corresponding to maximal value of molar heat capacity, Δc_p, in Figure 1.
Subscript 1 corresponds to the first N-to-I transition, and subscript 2 corresponds to the subsequent I-to-D process.

Table S2. Parameters obtained from DSC transitions of CcO at indicated concentration of CcO at scan rate 1.5 K/min. The listed parameters (transition temperatures, T_x, are temperatures corresponding to maximal value of molar heat capacity and values of calorimetric enthalpies, ΔH_{ux}, correspond to surface under the corresponding DSC transitions) are experimentally determined values from DSC scans and are model-independent.

[CcO] *(μM)*	T_1 *(°C)*	ΔH_{u1} *(kJ/mol)*	T_2 *(°C)*	ΔH_{u2} **(kJ/mol)**	R^2
0.55	46.2±0.1	510±11	59.5±0.1	1236±12	0.9922
1.1	47.5±0.1	456±14	60.0±0.1	1270±14	0.9897
1.6	48.4±0.1	500±14	60.8±0.1	1169±15	0.9904
2.1	48.7±0.1	525±10	61.1±0.1	1271±9	0.9953
3.2	50.3±0.1	454±6	61.5±0.1	1161±6	0.9981
3.6	50.6±0.1	463±17	61.4±0.1	1148±20	0.9789
4.1	51.6±0.1	461±16	61.2±0.1	1235±19	0.9850
5.0	51.6±0.1	504±11	61.6±0.1	1157±12	0.9917
5.2	51.0±0.1	481±15	61.8±0.1	1320±18	0.9914

Subscript 1 corresponds to the first N-to-I transition, and subscript 2 corresponds to the subsequent I-to-D process.

Table S3. Calculated parameters based on two-step analysis of the data shown in Figure 7 the irreversible thermal transitions of PL-containing CcO's (5 μM) in the presence and the absence of 2mM sodium cholate in different concentrations of dodecyl maltoside (DM).

[DM]±cholate	E_{a1} **(kJ/mol)**	T_1^*/T_1 **(°C)**	ΔH_{u1} **(kJ/mol)**	$\tau_{37\ degC}$ **(hours)**	E_{a2} **(kJ/mol)**	T_2^*/T_2 **(°C)**	ΔH_{u2} ***(kJ/mol)***	R^2
2mM -cholate	354	53.0/51.6	504	7.3	413	63.2/61.6	1157	0.9907
	±13	±0.2	±13		±6	±0.1	±15	
6mM -cholate	359	50.9/49.8	448	4.5	384	62.5/61.0	1245	0.9965
	±7	±0.1	±7		±3	±0.1	±8	
10mM-cholate	346	50.5/48.8	459	3.2	419	62.0/60.8	1187	0.9964
	±7	±0.1	±7		±4	±0.1	±8	
14mM-cholate	347	49.6/48.0	465	1.5	409	61.9/60.8	1195	0.9954
	±8	±0.1	±8		±4	±0.1	±9	
2mM +cholate	526	54.1/54.3	280	475.0	320	63.8/61.1	1079	0.9820
	±24	±0.1	±11		±9	±0.1	±15	
6mM +cholate	406	52.6/52.1	415	22.0	381	62.8/60.9	1280	0.9815
	±22	±0.2	±17		±8	±0.1	±22	
10mM+cholate	375	51.7/50.7	408	8.2	419	61.4/60.0	1112	0.9898
	±14	±0.1	±12		±6	±0.1	±13	
14mM+cholate	361	51.5/50.2	419	6.1	423	61.5/60.3	1122	0.9966
	±8	±0.1	±7		±4	±0.1	±8	

*T** values are the temperatures at which the rate constant for the specific reaction is 1/min. *T* values are the temperatures corresponding to maximal value of molar heat capacity, Δc_p, in Figure 7.

Subscript 1 corresponds to the first N-to-I transition, and subscript 2 corresponds to the subsequent I-to-D process.